



Published in final edited form as:

Ann Biomed Eng. 2018 October ; 46(10): 1479–1497. doi:10.1007/s10439-018-2075-x.

MRI Robots for Needle-Based Interventions: Systems and Technology

Reza Monfaredi^{1,*}, Kevin Cleary¹, and Karun Sharma^{1,2}

¹Sheikh Zayed Institute for Pediatric Surgical Innovation, Children's National Health System, 111 Michigan ave. NW, Washington, DC 20010

²Diagnostic Imaging and Radiology Department, Children's National Health System, 111 Michigan ave. NW, Washington, DC 20010

Abstract

Magnetic resonance imaging provides high-quality soft-tissue images of anatomical structures and radiation free imaging. The research community has focused on establishing new workflows, developing new technology, and creating robotic devices to change an MRI room from a solely diagnostic room to an interventional suite, where diagnosis and intervention can both be done in the same room. Closed bore MRI scanners provide limited access for interventional procedures using intraoperative imaging. MRI robots could improve access and procedure accuracy. Different research groups have focused on different technology aspects and anatomical structures. This paper presents the results of a systematic search of MRI robots for needle-based interventions. We report the most recent advances in the field, present relevant technologies, and discuss possible future advances. This survey shows that robotic-assisted MRI-guided prostate biopsy has received the most interest from the research community to date. Multiple successful clinical experiments have been reported in recent years that show great promise. However, in general the field of MRI robotic systems is still in the early stage. The continued development of these systems, along with partnerships with commercial vendors to bring this technology to market, is encouraged to create new and improved treatment opportunities for future patients.

Keywords

Literature survey; magnetic resonance imaging; robots; diagnostic; interventional; procedures

I. Introduction

Magnetic resonance imaging (MRI) is a well-established diagnostic tool in medicine. MRI provides excellent soft-tissue images of anatomical structures. Unlike computed tomography (CT) or fluoroscopy, MRI does not expose patients to ionizing radiation, which is especially important in the pediatric population.

* rmonfare@cnmc.org, Telephone no.: (443)240-8998.

MRI capabilities have improved in the past 10 years to enable needle-based interventions in a typical closed bore scanner. Using MRI, a physician can select a target and introduce a needle through the skin to targeted anatomical structures such as the joint space or nerve roots to inject contrast agent or pain medicine. The physician can also reach different internal organs, such as prostate, breast, liver, and brain to perform biopsy and to target cancerous lesions with needle-based ablation procedures to burn or freeze malignant cells.

The vast majority of diagnostic MRI scanners are closed bore scanners with bore diameters around 60 cm. Patient access in a closed-bore MRI scanner is challenging because working in the bore is ergonomically difficult due to the limited space available. Therefore, the patient needs to be moved in and out of the scanner for imaging and needle placement. Hand to eye registration based on 2D MR images is another characteristic of manual needle-based MRI-guided intervention. Therefore, MRI safe and MRI conditional robots have been introduced by the research community to improve access and procedure accuracy.

The high magnetic field present in the MRI environment, interaction with radiofrequency (RF) signals, and switching gradients are major challenges in developing MRI robots. In recent years, the research community has focused on establishing new workflows, developing new technology, and creating robotic devices to change an MRI room from a solely diagnostic room to an interventional suite, where diagnosis and intervention can both be done in the same room.

Different research groups have focused on different technology aspects and anatomical structures. This paper presents the results of a systematic search of MRI robots for needle-based interventions. We report the most recent advances in the field, present relevant technologies, and discuss possible future advances.

The term MRI-compatible was historically used to describe robots developed for the MRI environment, but it is no longer used and is now obsolete. Therefore in this paper we use the new terminology of ASTM standard F2503–13, as described in Section IV, where the terms MRI safe and MRI conditional are introduced. In this paper the term “MRI robot” is used to represent both MRI safe and MRI conditional robots.

II. Methods

We used the Google Scholar database since it includes scholarly articles from a wide variety of sources in all fields of research, all languages, all countries, and over all time periods. A recent study estimated the size of Google Scholar at 100 million documents as of September 2014, which covers about 88% of all scholarly documents accessible on the Web in English [1].

We systematically searched Google scholar papers by title using the keywords in Dataset A. Then we applied a year range filter to limit the search range. We used the exclusion criteria listed in Dataset B to delete unrelated papers:

$$\text{Dataset A} = \{\text{MR Robot, MRI Robot, MRI robotics, Magnetic Resonance Robot}\}$$
$$\text{Dataset B} = \{\text{Mister robot, MR fluid, Mobile Robot(MR), preoperative MR}\}$$

A staff scientist, with 6 years of experience in MRI robotics, evaluated the search results to ensure all inclusion and exclusion criteria were applied properly. Figure 1 shows the search progress. The last comprehensive MRI review paper was published in 2007 [2]. Therefore we focused in the time interval between 2008 and 2017 and found 307 papers. After applying the exclusion criteria in Dataset B, this number was reduced to 230 papers. For papers focused on prostate application we applied another filter (papers published in the last five years) to further limit the number of the papers. If there were multiple papers from the same research group, we focused on the most recent publications.

The remainder of the paper is organized as follows. In section III, MRI robots is presented through the different applications areas. Section IV focuses on technology components of MRI robots. Section V discusses the progress in the field and the future of MRI robots.

III. MRI robots applications

MRI is the preferred imaging modality for evaluation of soft tissue since it provides excellent intrinsic soft tissue contrast and also avoids ionizing radiation. Some of the uses for MRI are investigation and diagnosis of [3]: 1) abnormalities of the brain and spinal cord, 2) tumors, cysts, and other abnormalities in various parts of the body, 3) injuries or abnormalities of the joints and spine, 4) structural heart defects, 5) diseases of the liver, kidney, and other abdominal organs, 6) pelvic pain in women, and 7) suspected uterine abnormalities in women undergoing evaluation for infertility. This paper focuses on some of the applications of interest to the robotic research community. In the following subsections, MRI robotic systems for needle-based interventions are discussed under four different topics: 1) prostate biopsy and brachytherapy, 2) brain biopsy and intervention, 3) breast cancer diagnosis and intervention, and 4) other MRI-guided needle-based interventions.

A. Prostate biopsy and brachytherapy

Prostate cancer is the most common male cancer and the second leading cause of cancer death in men in the U.S. [4]; one-quarter of new cancer diagnoses in men are prostate cancer [5]. Siegel et al. estimated 220,800 new cases were diagnosed and almost 27,540 men died from prostate cancer in 2015 [5].

The most common way of diagnosing prostate cancer is the transrectal ultrasound (TRUS)-guided prostate biopsy, where an ultrasound probe is placed in the rectum to provide visualization of the prostate to guide the needle placement. There is also the transperineal approach where needles are placed through the perineum (the area behind the scrotum and in front of the anus). A brachytherapy grid is placed over the perineum to allow accurate placement of the biopsy needle within the prostate, together with the use of an ultrasound probe to direct the urologist.

TRUS-guided prostate biopsy is relatively blind to the location of cancer in the prostate, leading to many men without clinically important cancers undergoing potentially unnecessary biopsy. In addition, TRUS provides relatively low quality images of the tissue and needle. Therefore, this method frequently fails to detect clinically significant prostate cancer [6] [7].

MR imaging can provide detailed images with better anatomical visualization of the soft tissues of the prostate and can be useful in diagnosis and staging of cancerous lesions [6] [8]. To improve upon this capacity, robotic devices have been developed to assist in targeting suspicious lesions using pre-operative MR images fused to ultrasound images (MRI-ultrasound fusion method) [9] [10]. However, the prostate position could change in each subsequent MR imaging session, causing shift and error in fusion between ultrasound images and MR images. Interactive intraoperative MRI-guided prostate biopsy is an alternative method to the MRI-ultrasound fusion method, to eliminate errors associated with image registration and fusion. Manual needle-based targeting using intraoperative MR images is difficult due to the small confined space inside the MRI scanner and the need for hand to eye coordination of the interventionalist based on 2D MRI. Therefore, MRI robots have been introduced to enable intraoperative imaging guidance and automatic targeting.

Table 1 reports selected robotic systems from the last 5 years. More than 25% of the 230 published papers between 2008 and 2017 are focused on the prostate, making it the most popular clinical application. Therefore, we only reported papers published in the last 5 years in this table. This table is organized based on the study type and publication year. For each paper, research team, study type (i.e. phantom study; animal study; and clinical study), accuracy, DOF, actuation type, control type, signal to noise ratio (SNR), design, and institute are indicated, where available. For multi-institutional projects only the first institute is depicted in the summary tables.

The earliest work for MRI-guided prostate intervention robots was performed at Brigham and Women's Hospital in collaboration with the Agency of Industrial Science and Technology/ Ministry of International Trade and Industry (AIST-MITI, Ibaraki, Japan) [11]. In this project, a robotic intervention assistant was constructed for open MRI to guide needles and probes during prostate biopsy and brachytherapy. Since a clinically significant tumor has > 0.5 ml volume, corresponding to a sphere with diameter 9.8 mm, an MRI guided biopsy system employing a targeting accuracy of 5 mm or better could reliably access clinically significant prostate cancer foci [12].

Since then, several different MRI robotic systems have been developed. However, only a few systems have reached clinical application. The first human trial using an intraoperative-MRI-guided robotic system was reported by Bosch et al. on one patient [13]. This system had 5 DOF of manually-adjustable passive motions and 1 DOF of pneumatically-driven automatic needle drive. During the needle insertion fast 2D images were generated to track the needle on-line. All fiducial gold markers were delivered inside the prostate successfully.

About the same time Xu et al. utilized the system developed in [14] to perform MRI-guided focal laser ablation in 21 patients with prostate cancer. A mean biopsy error of 4 mm with a standard deviation of 2 mm was achieved in this study [15]. Böstrom et al. reported an in-bore robotic MRI-guided laser ablation of prostate cancer with 3 mm accuracy and applied to two human subjects who were discharged home the same day. The ablation resulted in greater than 90% destruction of the target in either the immediate or 1 week post treatment scan [16].

Another group in the Netherlands [17] developed a 5-DOF pneumatically-actuated robotic system and tested it on 13 subjects. The mean biopsy error was larger when using the robotic technique versus manual technique (6.5 mm vs 4.4 mm). Mean procedure and manipulation time were 76 min and 6 min, respectively using the robotic technique and 61 min and 8 min with the manual technique.

Srimathveeravalli et al. at Johns Hopkins [19] developed a 3-DOF robotic system using MRI safe stepper motors (PneuStep [20]), specifically developed for the MR environment. A six-animal study showed targeting accuracy of 2.58 mm with standard deviation of 1.31 mm for 30 targeting attempts. Normalized SNR of this system was reported as 9.99 with standard deviation of 2.88.

Ball et al. [18] used a 6-DOF robotic system called MrBot (Figure 2) to complete an IRB-approved human trial. Five men with mean age of 66.4 years underwent biopsy with MrBot. A prior negative 12-core biopsy was reported for these patients. For 30 biopsy sites, a targeting accuracy of 2.55 mm, with no trajectory corrections and no unsuccessful attempts, was reported. All patients tolerated the procedure well. The result of biopsy for the first patient was false-negative due to use of semi-automated biopsy needle that resulted in large deformation of the needle and missing the lesion. For the next four patients, this needle was replaced with a fully automated biopsy needle and rotated 180° about its axis, near the midpoint of the insertion stroke, to compensate for the lateral deformation of the needle. Targeting attempts were successful for these cases. Biopsies showed the presence of a clinically significant cancer in 2 patients. The biopsy results for the other two patients revealed no clinically significant cancerous lesions.

Chen et al. [22] tested a 2 DOF pneumatic system in a canine cadaver study. They reported an accuracy of 0.9 mm with a standard deviation of 0.4 mm. Other research groups have been developing MRI robot for prostate cancer interventions that are in the phantom study phase [21]-[34]. Figure 3 shows one of these systems called MIRIAM robot [21]. The MIRIAM robot is actuated by piezoelectric motors, while the needle insertion mechanism is actuated by a pneumatic motor.

Yiallouras et al. [32] developed a 3 DOF robot for manipulating a high-intensity focused ultrasound (HIFU) system to treat prostate cancer transrectally. HIFU is a method of delivering ultrasonic energy to generate heat to destroy cancerous lesions without damaging healthy tissues in the ablation region [35]. Unlike robotic-assisted radiation therapy using CyberKnife [36], robotic-assisted HIFU provides a radiation-free method for lesion ablation. One major drawback of HIFU is its inability to reach regions where there are air cavities along the path of the beam, since ultrasound waves are dispersed and poorly transmitted in air [37].

B. Brain biopsy and interventions

Brain related procedures include biopsy, injection of drugs, laser surgery, radiation treatment, and positioning of electrodes for deep brain stimulation [38]. Unlike prostate biopsy, due to the thick skull encompassing the human brain, the use of ultrasound imaging is limited in neurosurgery. CT imaging does not provide high contrast images of the soft

tissue of the brain while it exposes the patient to ionizing radiation. MRI is also the most widely used imaging modality that can visualize both the function and structure of the brain.

There has been some development of needle intervention systems and even surgical robot systems for brain interventions. There are multiple commercially available passive MRI safe devices including NexFrame[®] (Medtronic, Inc, USA) [39], Visualase[®] (Medtronic, Inc, USA) [40], NeuroBlate[®] (Monteris Inc., USA) [41], and ClearPoint[®] (MRI Interventions, Inc., USA) [42]. These devices can improve the targeting procedure in neurological procedures compared with conventional manual methods. However, they are passive devices and rely on the performance of the operator which leads to subjective accuracy of the system. In addition, manual adjustment of the position and orientation of the frame is non-intuitive and time-consuming [43]. The non-MRI compatible NeuroMate robot (Renishaw Inc., United Kingdom) was used in a clinical study of 51 patients with an accuracy of 1.7 mm for DBS electrode placement using pre-operative MRI. Many cases required several insertion attempts and errors due to brain shift and only 37 of 50 targeting attempts were successful [44]. Using intraoperative MRI for locating the target point and using an MRI-compatible robotic needle guide can also minimize brain shift issues after opening the skull.

An MRI robot with automatic registration capability could provide repeatable and accurate positioning during neurosurgical procedures with minimal inter-surgeon variability. In addition, interactive MRI-guided visualization of brain while advancing the probe toward the target lesion could increase accuracy and safety. Masamune et al. pioneered an 6 DOF stereotactic neurosurgical MRI robot. This robotic system was tested on a 0.5 Tesla Hitachi MRI scanner with accuracy of 3 mm on a watermelon [38]. Since then, different research groups focused on MRI robotic systems for neurosurgical procedures in the last ten years as shown in Table 2.

Lang et al. [45] developed the NeuroArm robot driven by piezoelectric motors with dual dexterous arms for MR-guided stereotaxy and microsurgery. The end-effector was designed to hold various surgical devices such as micro scissors, bipolar forceps, a suction device, and needles. This system was used in 35 neurosurgical patients. The surgeons used a graded approach to introduce the NeuroArm into surgery, with routine dissection of the tumor-brain interface occurring over the last 15 cases [46]. Figure 4 shows the NeuroArm robot in a MRI room.

A finger-like neurosurgery robot was developed at the University of Maryland using shape-memory-alloy actuators [47]. This technology has a very limited bandwidth [43]. The same research group proposed a new design over their previous design [47] that uses a spring-based backbone with three segments. These independently actuated segments are used instead of previously used rigid links to provide more maneuverability and compliant interface. Compressed air cooling is utilized to increase the actuation bandwidths [48].

Comber et al. [49] presented a pneumatically actuated robot for MRI-guided neurosurgery. The concentric tube structure of the robot resulted in inherent nonlinearity and control challenges. This robotic system was later adapted for treating epilepsy via thermal ablation [50] and for transforaminal hippocampotomy [51]. Li et al. [43] developed a 5 DOF robot

plus a manual cannula guide for MRI-Guided Stereotactic Neurosurgery which is kinematically equivalent to a Leksell frame. The SNR was investigated in three configurations: 1) difference between baseline and robot present but unpowered, 2) difference between robot present but unpowered and robot powered, and 3) difference between robot powered and robot running. The mean SNR reductions from baseline for these configurations were 2.78%, 6.30%, and 13.64% for T1 weighted and 2.56%, 8.02%, and 12.54% for T2 weighted imaging, respectively. The tip position RMS error was 1.38 mm and angular error was 2.03° for the six targets. A new version of this robot was introduced in [52] which is shown in Fig. 5. This research group has conducted new experiments recently to evaluate their system's accuracy and repeatability as a final step toward pre-clinical trials [53].

Heikkila et al. developed a 6 DOF robot for a 0.23 Tesla magnet [54]. The low magnetic field for the MRI scanner allowed the use of shielded servomotors in the MRI room. Su et al. modified a previously designed robotic system for a prostate biopsy procedure [55] to create a reconfigurable MRI-guided surgical manipulator adapted to neurosurgery applications [56].

C. Breast cancer diagnosis and intervention

Breast cancer is the most common cancer in women after lung cancer. 12.5 % of women in the USA experiences breast cancer in their lifetime. In the USA alone, about 266,120 new breast cancer cases will be diagnosed in 2018 [57]. Worldwide, nearly 1.7 million incidence of breast cancer were reported in 2012, and the incidence worldwide is increasing [58].

Mammography is the standard for breast cancer detection and diagnosis. Biopsy of suspicious masses is then done under ultrasound (US) or MRI guidance. Mammography exposes the patient to ionizing radiation. Therefore, women aged 30s are not recommended to undergo regular mammogram screenings. In addition, only the shape and density of lesions could be detected by mammogram images, and not the tissue characteristics of the high-risk lesions [59]. Among imaging modalities, MRI is highly sensitive to breast cancer lesions. This imaging modality provides a detection rate around 90% and therefore is recommended for high-risk patients as a complementary approach to mammography, ultrasound, or palpation [59].

Currently, several MRI-guided free-hand or stereotactic devices have been developed for breast biopsy interventions [60]. These devices have several drawbacks. First, most of the devices provide breast compression along a specific direction, which may not be optimal since they often do not provide the shortest path to target. Second, in most of the devices the needle is guided using a grid mesh, and thus it can only be inserted perpendicular with a slight pitch with respect to the compression plates [60]. Third, for using these devices the patient is moved in and out of the magnet, to insert the biopsy needle and to obtain a confirmation scan [60]. To address these limitations of the currently available MRI safe biopsy devices, MRI robotic systems have been investigated by the research community.

The first robotic system for biopsy and therapy of breast lesions was introduced by Kaiser et al. [61] in 2000. Larson et al. developed the first surgical robotic device for interactive MRI-

guided breast intervention in the United States [60]. Since then, several new systems have been reported in the literature. MRI robotic systems developed in the last 10 years are listed in Table 3. Yang et al. [62] used pneumatic cylinders to develop a master–slave breast biopsy robotic system to work in MRI. This system uses a 6 DOF robotic platform including a 1 DOF needle driver to perform a localization procedure for biopsy. Figure 6 shows the slave robot on a MRI scanner table. This robotic platform requires opening the breast coils toward the face.

Animal studies were done to test the overall system performance, but additional work is needed to move towards clinical application as noted by the authors.

The IGAR (Image-guided Automated Robot) is a robotic system developed by Chan et al. [63] for breast biopsy. The system was tested in air and accuracy and repeatability of 0.34 mm and 0.2 mm were reported [63]. Zhang et al. developed a palm-shape breast deformation device designed to actively reshape the breast and immobilize it for manual intervention. This device could be actuated inside the magnetic bore with image feedback [64]. Park et al. developed an automated bendable needle intervention robotic system for MRI-guided breast biopsy to overcome the space limitation of the scanner bore [59]. This robotic system allows accessing the breast area from the side of a patient. Fig. 7 shows a photograph of this robotic system and the setup. The surgeon picks a target point from the MR images and the robotic system calculates the needle's navigation, visualizes the needle path, and automatically drives the bendable needle in a curved trajectory to the target. Phantom studies showed 0.8 mm accuracy for locating the needle tip [59]. Although, several active research teams have developed MRI-guided robotic intervention systems for the breast, no clinical trial has been reported to the best of our knowledge.

Navarro-Alarcon et al. [65] developed an MRI compatible compact robot with (semi-) automatic needle driver. This system is developed to perform both frontal and lateral needle insertion inside the MRI bore. It also could be used to perform lateral automatic needle insertion in an open bore MRI (such as PICA Scanner developed by Time Medical). This system is a 3 DOF system. 2 degrees of freedom for aligning the needle guide toward the targeted lesion and 1 DOF for needle insertion. Initial positioning of the needle guide tip should be done manually using grids before switching to automatic mode. A robust feedback controller was suggested by the authors for pneumatic-based needle insertion motion. The phantom study showed ± 1.5 mm insertion accuracy for this system. Groenhuis et al. [66] developed a novel and compact 4 DOF robotic system using linear pneumatic stepper motors and a novel curved pneumatic stepped motors. In air accuracy study showed positional accuracy of 0.71 mm, 0.2 mm and 0.21 mm accuracy in x, y and z directions. Zhang et al. [67] developed a 5 DOF MRI robot with 3 DOFs for the needle guide in x, y, and z directions. It has an extra DOF for avoiding the obstacles (grid plates) and one DOF for the puncturing module for inserting and withdrawing the needle. This robot has a storage module to collect biopsy samples. Forward and backward analysis and results for phantom study for smooth motion and accurate positioning of the robot has been reported in this paper.

D. Other MRI-guided needle-based interventions

Many CT-guided needle-based interventional procedures could be done under MRI to avoid ionizing radiation and provide better soft tissue contrast.

Table 4 shows various robotic systems developed for MRI-guided needle-based intervention. The last column of the table indicates the application area. These systems are briefly discussed below.

While CT imaging is typically better for bone imaging, for biopsy of bone and adjacent soft tissue such as bone marrow and periosteum, MRI has some advantages. Bone infections and cancers are soft and conventional radiographs may appear normal, especially in the early course of disease. MRI is often used to aid in the diagnosis due to its improved soft tissue, marrow, and joint space resolution [70].

Monfaredi et al. [68] [69] developed a patient-mounted robot for shoulder arthrography as shown in Fig. 8. Arthrography is the evaluation of joint condition using imaging modalities. Currently, this test requires two separate stages, an intra-articular contrast injection guided by fluoroscopy or ultrasound followed by an MRI. The manual nature of needle placement can lead to increased cost, anxiety, and in some cases prolonged sedation time. This patient-mounted robot could streamline the workflow from a two-room procedure to an MRI-room only procedure. Kim et al. [71] developed a new generation of their previous patient-mounted robot using parallel architecture that initially aimed for shoulder Arthrography. This robot also has 4 DOFs for positioning and orienting the needle guide. Two identical circular stages are placed on top of each other as a sandwich platform to provide a 4 DOF robot. This new design provides increased rigidity, and lower moment of inertia due to non-moving components attached to the base. In this design motors and encoders are attached to the base and motor and encoder cables are fixed resulting in less interference of the cables with the robot.

Stoianovici et al. [72] developed a MRI robot for bone biopsy as shown in Fig. 9. A phantom study showed an average 2D targeting error of 1.25 mm and an average 3D error of 1.39 mm. The standard deviation was 0.39 mm for 2D and 0.40 mm for 3D. Squires et al. [73] developed an MRI-guided needle positioning robot called SpinoBot for spinal cellular therapeutics using pneumatic turbine motors. A SpinoBot test in swine cadaver resulted in a mean error of 2.2 mm and standard deviation of 0.85 mm. Less than 3% SNR reduction under 3 Tesla MR imaging was reported.

Recently, a non-survival study on eight swine using an Innomotion system, a general percutaneous intervention robot developed by Melzer et al. [74], was conducted to show the feasibility of interactive MRI-guided transcatheter aortic valve replacement [75]. Previously, Li et al. [76] also utilized an Innomotion system with an embedded 3 DoF valve delivery module for MRI-guided insertion of aortic valve prostheses. The physician uses interactive control and MRI feedback to adjust the orientation and position of balloon and stented prostheses with accuracy of 1.5 mm and 0.8 mm, respectively.

Only in the U.S., 1,059,000 new case of cardiac catheterizations are performed annually. Percutaneous transluminal catheter procedures conventionally rely on fluoroscopic X-ray. Exposing both patients and staff to radiation, low tissue contrast, 2-D projections of the anatomical site interactively, and difficulty of hand to eye coordination are some of the limitations of conventional approach. Tavallaei et al. [77] developed a 2 DOF master-slave catheter navigation system to facilitate intraoperative MRI-guided catheterization procedures.

Franco et al. [78] [79] developed a pneumatically actuated table-mounted robotic system to assist clinicians in MRI-guided liver tumor ablation and to assess liver functionality in a clinical setting. This robotic system underwent two clinical studies with promising outcomes. Percutaneous ablation of liver tumors using a catheter has been tested under MRI guidance. Phantom experiments suggested potential time saving while using this needle-guiding MRI robot to be 30 minutes for single-lesion liver ablation procedures.

IV. Technologies for MRI robots and MRI-guided interventions

The high magnetic field present in the MRI environment, interaction with radiofrequency (RF) signals, and switching gradients are major challenges in developing MRI equipment. A great deal of precaution is therefore required when working in the MRI environment. The standard F2503–13 of the American Society of Testing and Materials (ASTM) categorizes devices in the MRI environment to three different classes from a safety perspective [80]: 1) *MR Safe*: an item that poses no known hazards resulting from exposure to any MR environment, 2) *MR Conditional*: The device when used in a specified MR environment with specified conditions of use poses no known hazards to the patient or medical team, and 3) *MR-Unsafe*: an item which poses unacceptable risks to the patient, medical staff or other persons within the MR environment. Figure 10 shows the standard icons for labeling of equipment in the MRI environment.

Nonmagnetic materials, MRI safe/conditional actuators, optical encoders, and force sensors are key elements of robotic systems for the MRI environment. 35% of the publications focused on technology in general, meaning that no specific application was highlighted as the primary goal of the study. In this section, different technology components for MRI robots are discussed, including MRI safe/conditional materials, actuators, and force sensing, along with registration techniques and shielding issues.

A. MRI safe/conditional materials

Ferromagnetic materials have to be avoided entirely in the MRI room because they cause image artifacts and distortion due to field inhomogeneity, and they pose a dangerous projectile risk to the patient and medical team. Non-ferromagnetic metals such as aluminum, brass, titanium, high strength plastic, and composite materials are compatible with MRI environment. However, the use of any conductive materials in the vicinity of the scanner's isocenter must be limited because of inducing eddy currents, deforming the magnetic field homogeneity, and as a result imposing noise and artifacts to MR images. Electrical systems must be properly shielded and filtered, to limit noise emission. While designing the system more considerations should also be taken to avoid resonance and heating [81]. From a risk

point of view, eddy currents may heat up the materials, posing a danger to the patient. Therefore, all cables that come in direct contact with patient's skin should be covered. For materials that come in direct contact with the patient's tissue or needle, such as a needle-guide, they should be constructed from certified biocompatible material (ISO-10993). Techniques for evaluation and quantification of force and torque applied by MRI machine to MRI robots could be found here [82].

B. MRI safe/conditional Actuators

The choice of a proper actuator and drive system is a main challenge while designing a robot for MRI environment. In addition to MRI compatibility criteria, this choice depends largely on the task, required output power, maximum force, speed, and acceleration as in a traditional design [83]. To date, a wide variety of non-magnetic motors have been introduced that are MR safe or MRI conditional [81]. Gassert et al. [83] investigated different types of actuation options for the MRI environment and discussed advantages and limitations. There are 5 main types of actuators that could be used in MRI environment [83]: 1) mechanical actuation and transmissions, 2) pneumatic actuators, 3) hydraulic actuators, 4) electric actuators (including piezoelectric/ultrasonic actuators, electrostatic actuators, electro-active and Ion conducting polymers, and electrorheological fluid brakes), and 5) electromagnetic actuators (including lorentz actuators/magnetomechanical vibrotactile devices, and shielded DC motor). In addition, an investigation into the MRI compatibility of different actuators during an fMRI study was reported in [84]. Fischer et al. [85] investigated the three most common type of actuators from an image quality point of view.

Our literature review shows that piezoelectric/ultrasound motors and pneumatic actuators are the most popular actuation types in MRI systems built to date. Recently, shape memory alloy (SMA) technology also has been adapted to develop robotic systems for MRI environment [47]. Chen et al. [31] developed a 5 DOF robotic system using novel pneumatic motors. Each motor consist of a rotor with conical holes and multiple pistons with conical tip and one-third phase difference. Vartholomeos et al. [86] developed MRI-powered actuation technology. In this novel approach, the MRI scanner is used to deliver power. It also could be used to estimate actuator state and to perform closed-loop control. MRI-powered actuators proposed by Ouchi et al. [87] utilize the gradient switching magnetic field of MRI room to actuate the system. All parts of this MRI-powered actuator are non-magnetic except for the sphere embedded in the rotor. The pendulum movement of the ferromagnetic rotor is converted to translation, generating linear motion.

C. MRI safe/conditional position sensors and force sensors

Fiber optic based position and force sensors have been developed that are compatible with the MRI environment. Optical encoders are typically used to read and transmit the relative position of rotary shafts or linear stages. Fiber Bragg grating sensors can be used to read and transmit external force and torques which are proportional to deformations in a force/torque sensor [88]. Multiple off-the-shelf optical encoders are available for developing MRI robots. Signals should be transmitted through shielded, twisted pair cables to the encoder interface [43]. Extra shielding for the embedded electronic board of these encoders can reduce the noise-induced drop [89]. To the best of our knowledge, there is no commercial MRI safe or

MRI conditional force sensor available in the market. However, a review paper covering custom-made MRI safe or MRI conditional force sensors has been published recently [90]. This paper focused on fiber-optic based force sensors for interventional applications and rehabilitation devices.

D. Electronic equipment shielding

The American College of Radiology has defined four safety zones within MRI facilities corresponding to levels of increasing magnetic field exposure and safety concerns, denoted as Zones I through IV [91]. Zone I refers to all areas freely accessible to the general public without supervision. Zone II is the interface area between the unregulated Zone I and the strictly controlled Zones III and IV considered for MR safety screening. Zone III is an area near the magnet room where the fringe, gradient, or RF magnetic fields are very strong and unshielded patients and personnel are not allowed in this zone. However, unshielded electronics and devices are allowed in Zone III. Zone IV is the MRI scanner room and any of ferromagnetic objects must be excluded from this room. This room is heavily shielded and separated from Zone III by a patch panel.

Any electrical communication between Zone III and Zone IV should go through the patch panel. The patch panel is a metal shielded panel, typically made out of copper, for routing electrical signals. The patch panel usually incorporates at least one waveguide (metal tubes) for routing fiber optic cables, pressure tubes, and other non-conductive cabling. Poor shielding of robots with electric wires in the MRI scanner room results in MRI image degradation and SNR drop while the robot is powered. All motor drivers and other essential electronics in the scanner room should be placed inside a Faraday cage with proper non-ferromagnetic metal connectors to seal the enclosure box. The SNR drop while powering and running piezoelectric motors could potentially be improved with special drivers and additional shielding [92].

E. Registration methods and MRI robot system evaluation

Accurate targeting during MRI-guided procedures requires precise calibration and registration of the robot's coordinate system with the MRI coordinate system. Different registration techniques using both active and passive fiducials have been proposed [14] [93]. Active fiducial-based registration is associated with higher accuracy and faster registration. However, it requires special scanner programming, and dedicated scanner channels. Using an image-based passive registration approach, expensive coil and dedicated scanner channels are not required. Shang et al. [94] presented a multi-image based passive registration method, known as Z-frame registration. The fiducial frame represents a cube with 7 embedded MR visible tube fiducials (Beekley, Bristol, CT) in a Z-shape arrangement. This method provides better accuracy compared to single-image based registrations.

An automatic calibration method was presented by Tokuda et al. [95] using the Z-frame approach. This method automatically identifies fiducial markers without operator intervention. The design of user interface and workflow management were based on clinical workflow analysis of MRI-guided prostate intervention that consists of three subsystems: (a) Needle placement robot controller, (b) Closed-bore MRI scanner's control software, and (c)

3D slicer as an open-source surgical navigation software (3D Slicer, <http://www.slicer.org>) [95] [96]. 3D Slicer as the core component of the software system, creates an integrated environment for calibration, surgical planning, image guidance and device monitoring and control. A software module in 3D Slicer was also created to offer all required features for MR-guided robotic needle-based interventions [93]. Stoianovici et al. [97] proposed a comprehensive set of tests to evaluate the MRI robotic systems synthesized based on international standards, their experience building MRI robots, and inputs from the FDA approval process of a MRI safe robot.

V. Discussion and Conclusion

MRI has some unique characteristics for image-guided interventions, including excellent soft tissue contrast, no ionizing radiation, the ability to study brain activity with functional MRI, and accurate detection, characterization, and staging of cancerous lesions using multi-parametric MRI. MRI technology continues to advance and is changing from a solely diagnostic tool to both a diagnostic and an interventional tool. MRI can be used during needle-based interventions to track the needle tip interactively and to acquire continuous visual feedback of the path and depth of needle insertion. To make MRI-guided procedures more accurate, MRI robots have been introduced to use intraoperative MR images for automatic needle-based targeting.

Although there have been substantial efforts to develop MRI robotic systems by the research community, translation to clinical practice has been slow. While there are many reasons for the slow pace of this translation, two major reasons are technical challenges and limited market demand. The research community has been working to solve the technical challenges and to develop new workflows for different applications as described in this review article. Researchers, especially in the university environment, would benefit from more access to the clinical environment and access to MRI facilities for technology evaluation purposes. They also need to be aware of regulatory aspects of medical research to facilitate translating research concepts to clinical practice.

As for market demand, many CT-guided needle-based interventional procedures could be performed with MRI guidance to avoid ionizing radiation and improve visualization. However, MRI is relatively expensive compared with other imaging modalities. Therefore, interventional procedures that require pre-operative MRI as part of the current workflow may be good candidates for intraoperative MRI-guided robotic interventions. Minimizing the time of the procedure in the MRI room is critical for realization of this technology and therefore workflow should be taken into account when developing a MRI robots.

Robotic-assisted MRI-guided prostate biopsy has received the most interest from the research community to date. In recent years, successful clinical experiments have been reported. However in general the field of MRI robotic systems is still in the early stage. It may still take time to overcome skepticism toward MRI robots because of the complexity of the devices and the currently unclear robotic procedure efficacy and value. As an example, the commercially available da Vinci robotic system was designed to facilitate complex surgery using a minimally invasive approach. Although this robotic system struggled

initially to gain market share, by strategically pivoting from the initial cardiac application to prostatectomy, it gained remarkable momentum commercial success. As of 2016, there was an installed base of 3,803 da Vinci robotic units worldwide, with 2,501 installed in the United States [98]. By providing surgeons with superior visualization, enhanced dexterity, greater precision, and ergonomic comfort, the da Vinci Surgical System has started a new era in robotic-assisted surgery.

As technology continues to advance, the idea of the digital operating room including robotic systems comes closer to realization. In that sense the robotic system could be considered an “information appliance” and part of the digital platform of the operating room of the future [99]. MRI robots could be part of this picture by enabling radiation free procedures with interactive imaging and superior soft tissue visualization.

With the increasing adoption of scanners with higher strength fields, the spatial resolution of the scanner and the imaging quality increases and the MR imaging time decreases. Shorter imaging sequences, along with faster segmentation techniques, registration algorithms, and streamlined setup could shorten the total procedure time and provide more cost-effective MRI-guided robot-assisted interventions, potentially leading to increased technology adaptation. Multi-parametric MRI is an emerging imaging modality for diagnosis, staging, characterization, and treatment planning of prostate cancer. These techniques could minimize the need for biopsy and shift the focus from performing biopsy procedures under MRI toward ablation procedures under MRI [100] [101].

Magnetic resonance guided robotic-assisted focus ultrasound enables noninvasive ablation procedures. It could also be combined with local drug delivery for tumor ablation in the future [102]. New systems with wider bores would provide more space for MRI robots. Stronger magnets will justify shifting toward purely pneumatic actuators to minimize the artifact induced by the stronger magnetic fields. Body coils and table coils with better signal reception could eliminate the need for coil positioned on the patient to free up this space for body-mounted or table-mounted MRI robots. Although in-bore treatments can improve the targeting and ablation accuracy, the increased costs associated with MRI-guided intervention is a drawback. Therefore, it will be important to minimize intervention time. Using MRI robots, especially in multi-target tumor biopsy and ablation, could significantly reduce the time, since after one time setup and robot to scanner registration, multiple targeting could be performed in a short period of time. Therefore the continued development of these systems, along with partnerships with commercial vendors to bring this technology to market, is encouraged to create new and improved treatment opportunities for future patients.

Acknowledgements:

This work was partially supported by the National Institutes of Health (NIH) under Grants R01EB020003, R01CA172244, and R21EB020700.

References

- [1]. Khabsa Madian, and Lee Giles C, “The Number of Scholarly Documents on the Public Web,” PLoS ONE, vol. 9, no. 5, 2014 e93949 10.1371/journal.pone.0093949. [PubMed: 24817403]

- [2]. “Tsekos NV, Khanicheh A, Christoforou E, and Mavroidis C, “Magnetic resonance-compatible robotic and mechatronics systems for image-guided interventions and rehabilitation: a review study,” *Annu Rev Biomed Eng*, vol. 9, pp. 351–387, 2007”. [PubMed: 17439358]
- [3]. <https://www.medicalnewstoday.com/articles/146309.php>.
- [4]. Center for Disease Control and Prevention. [Online]. <https://www.cdc.gov/cancer/dcpc/data/men.htm>
- [5]. Siegel RL, Miller KD, and Jemal A, “Cancer statistics, 2015,” *Cancer J. Clinicians*, vol. 65, pp. 5–29, 2015.
- [6]. Volkin D, Turkbey B, Hoang AN, Rais-Bahrami S, Yerram N, Walton-Diaz A, Nix JW, Wood BJ, Choyke PL, and Pinto PA, “Multiparametric magnetic resonance imaging (MRI) and subsequent MRI/ultrasonography fusion-guided biopsy increase the detection of anteriorly located prostate cancers. 1. 2014 Dec: 114:E43–9,” *BJU international*, vol. 114, no. 6b, pp. E43–E49, 2014. [PubMed: 24712649]
- [7]. HU Ahmed A Bosaily El-Shater, Brown LC, Gabe R, Kaplan R, Parmar MK, Collaco-Moraes Y, Ward K, Hindley RG, Freeman A, Kirkham AP, Oldroyd R, Parker C, and Emberton M, “Diagnostic accuracy of multi-parametric MRI and TRUS biopsy in prostate cancer (PROMIS): a paired validating confirmatory study,” *Lancet.*, vol. 389, pp. 815–822, 2017. [PubMed: 28110982]
- [8]. Hoeks CM, Barentsz JO, Hambrock T, Yakar D, Somford DM, Heijmink SW, Scheenen TW, Vos PC, Huisman H, van Oort IM, Witjes JA, Heerschap A, and Fütterer JJ, “Prostate Cancer: Multiparametric MR Imaging for Detection, Localization, and Staging,” *Radiology*, vol. 261, no. 1, pp. 46–66, 2011. [PubMed: 21931141]
- [9]. Chen K, Yuen J, Ho H, Cheng C, Lau K, LEE L, TAN Y, Law Y, and Tay K, “Robot-assisted transperineal MRI-ultrasound (MRI-US) fusion targeted biopsy is more efficacious in detecting clinically significant prostate cancer than systematic random saturation biopsy,” *International Journal of Urology*, vol. 23, pp. 64–65, 2016.
- [10]. Kaufmann S, Mischinger J, Amend B, Rausch S, Adam M, Scharp M, Fend F, Kramer U, Notohamiprodjo M, Nikolaou K, Stenzl A, Bedke J, and Kruck S, “First report of robot assisted transperineal fusion versus off target biopsy in patients undergoing repeat prostate biopsy,” *World Journal of Urology*, vol. 35, pp. 1023–1029, 2017. [PubMed: 27847972]
- [11]. Chinzei K, Hata N, Jolesz FA, and Kikinis R, “MR compatible surgical assist robot: system integration and preliminary feasibility study. Medical Image Computing and Computer-Assisted Intervention,” in *MICCAI 2000*, pp. 921–930.
- [12]. Mozer PC, Partin AW, and Stoianovici D, “Robotic Image-Guided Needle Interventions of the Prostate, 11(1): p.p. 7–15, 2009.,” *Rev Urol.*, vol. 11, no. 1, pp. 7–15, 2009. [PubMed: 19390670]
- [13]. Bosch MR, Moman MR, Vulpen M, Battermann JJ, Duiveman E, Schelven LJ, Leeuw H, Legendijk JJ, and Moerland MA, “MRI-guided robotic system for transperineal prostate interventions: proof of principle,” *Physics in Medicine and Biology*, vol. 55, pp. N133–N140, 2010. [PubMed: 20145293]
- [14]. Krieger A, Susil RC, Menard C, Coleman JA, Fichtinger G, Atalar E, and Whitcomb LL, “Design of a novel MRI compatible manipulator for image guided prostate interventions,” *IEEE Transactions on Biomedical Engineering*, vol. 52, no. 2, pp. 306–13, 2005. [PubMed: 15709668]
- [15]. Xu H, Lasso A, Vikal S, Guion P, Krieger A, Kaushal A, Whitcomb LL, and Fichtinger G, “Clinical Accuracy of Robot-Assisted Prostate Biopsy In Closed MRI Scanner,” in *The Hamlyn Symposium on Medical Robotics*, London, 2010, pp. 7–8.
- [16]. Boström Peter, Davidson Sean R. H., Lindner Uri, Raz Orit, Colquhoun Alexandra, Hlasny Eugen, Haider Masoom A., Mccluskey Stuart, Sussman Marshall, Yi Yang, Gertner Mark, and Kucharczyk Walter, “First Clinical Experience With Robotic Mr-Guided Focal Laser Ablation Of Prostate Cancer,” *Journal of Urology*, vol. 185, 2011.
- [17]. Schouten MG, Bomers JG, Yakar D, Huisman H, Rothgang E, Bosboom D, Scheenen TW, Misra S and Fütterer JJ, “Evaluation of a robotic technique for transrectal MRI-guided prostate biopsies,” *European Radiology*, vol. 22, no. 2, pp. 476–483, 2012. [PubMed: 21956697]
- [18]. Ball MW, Ross AE, Ghabili K, Kim C, Jun C, Petrisor D, Pan L, Epstein JI, Macura KJ, Stoianovici DS, and Allaf ME, “Safety and Feasibility of Direct Magnetic Resonance Imaging-

guided Transperineal Prostate Biopsy Using a Novel Magnetic Resonance Imaging-safe Robotic Device,” *Journal of Urology*, 2017.

- [19]. Srimathveeravalli Govindarajan, Kim Chunwoo, Petrisor Doru, Ezell Paula, Coleman Jonathan, Hricak Hedvig, Solomon Stephen B., and Stoianovici Dan, “MRI-safe robot for targeted transrectal prostate biopsy: animal experiments,” *BJU international*, vol. 113, no. 6, pp. 977–985, 2014. [PubMed: 24118992]
- [20]. Stoianovici D, Patriciu A, Mazilu D, Petrisor D, and Kavoussi L, “A new type of motor: pneumatic step motor,” *IEEE/ASME Trans Mechatronics*, vol. 12, no. 1, pp. 98–106, 2007. [PubMed: 21528106]
- [21]. Zandman Jonathan, Hekman Edsko E. G., van der Heijden Ferdinand, Borra Ronald, and Misra Sarthak, “The MIRIAM Robot: A Novel Robotic System for MR-Guided Needle Insertion in the Prostate,” *Journal of Medical Robotics Research*, vol. 2, no. 3, 2017.
- [22]. Chen Y, Xu S, Squires A, Seifabadi R, Turkbey IB, Pinto P, Choyke P, Wood B, and Tse ZTH, “MRI Guided Robotically Assisted Focal Laser Ablation of the Prostate Using Canine Cadavers,” *IEEE Transactions on Biomedical Engineering*, vol. PP, no. 99, 2017.
- [23]. Jiang S, Sun F, Feng W, Hofman LF, and Yu Y, “Analysis of a novel high-precision 5-degrees of freedom magnetic resonance imaging-compatible surgery robot for needle-insertion prostate brachytherapy,” *Proceedings of the Institution of Mechanical Engineers, Part C: Journal of Mechanical Engineering Science*, vol. 228, no. 5, pp. 865–876, 2013.
- [24]. Li G, Su H, Tokuda J, Hata N, Tempany CM, and Fischer GS, “A Fully Actuated Robotic Assistant for MRI-Guided Prostate Biopsy and Brachytherapy,” in *Proc SPIE Int Soc Opt Eng*, 2014.
- [25]. Su H, Camilo A, Cole GA, Hata N, Tempany CM, and Fischer GS, “High-Field MRI-Compatible Needle Placement Robot for Prostate Interventions,” in *Stud Health Technol Inform*, 2011, pp. 623–629. [PubMed: 21335868]
- [26]. Song S, Hata N, Iordachita I, Fichtinger G, Tempany C, and Tokuda J, “A Workspace-oriented Needle Guiding Robot for 3T MRI-guided Transperineal Prostate Intervention: Evaluation of In-bore Workspace and MRI Compatibility,” *Int J Med Robot*, vol. 9, no. 1, pp. 67–74, 2013. [PubMed: 22492680]
- [27]. Tokuda J, Song SE, Fischer GS, Iordachita I, Seifabadi R, Cho NB, Tuncali K, Fichtinger G, Tempany CM, and Hata N, “Preclinical evaluation of an MRI-compatible pneumatic robot for angulated needle placement in transperineal prostate interventions,” *Int J Comput Assist Radiol Surg*, vol. 7, no. 6, pp. 949–57, 2012. [PubMed: 22678723]
- [28]. Song SE, Cho N, Tokuda J, Hata N, Tempany C, Fichtinger G, and Iordachita I, “Preliminary Evaluation of a MRI-compatible Modular Robotic System for MRI-guided Prostate Interventions,” in *Proc IEEE RAS EMBS Int Conf Biomed Robot Biomechatron*, Tokyo, Japan, 2010, pp. 796–801.
- [29]. Krieger A, Song SE, Cho NB, Iordachita I, Guion P, Fichtinger G, and Whitcomb L, “Development and Evaluation of an Actuated MRI-Compatible Robotic System for MRI-Guided Prostate Intervention,” *IEEE/ASME Transactions on Mechatronics*, vol. 18, no. 1, pp. 273–284, 2013.
- [30]. Su H, Shang W, Cole G, Li G, Harrington K, Camilo A, Tokuda J, Tempany CM, Hata N, and Fischer GS, “Piezoelectrically Actuated Robotic System for MRI-Guided Prostate Percutaneous Therapy,” *IEEE ASME Trans Mechatron*, vol. 20, no. 4, pp. 1920–1932, 2015. [PubMed: 26412962]
- [31]. Chen L, Paetz T, Dicken V, Krass S, Al Issawi J, Ojdani D, Krass S, Tigelaar G, Sabisch J, Poelgeest AV, and Schaechtele J, “Design of a Dedicated Five Degree-of-Freedom Magnetic Resonance Imaging Compatible Robot for Image Guided Prostate Biopsy,” *J. Med. Devices*, vol. 9, no. 1, 3 01 2015.
- [32]. Yiallouras Christos, Ioannides Kleanthis, Dadakova Tetiana, Pavlina Matt, Bock Michael, and Damianou Christakis, “Three-axis MR-conditional robot for high-intensity focused ultrasound for treating prostate diseases transrectally,” *Journal of Therapeutic Ultrasound*, vol. 3, no. 2, 2015.
- [33]. Eslami S, Fischer GS, Song SE, Tokuda J, Hata N, Tempany CM, and Iordachita I, “Towards Clinically Optimized MRI-guided Surgical Manipulator for Minimally Invasive Prostate

- Percutaneous Interventions: Constructive Design,” in IEEE Int Conf Robot Autom, 2013, pp. 1228–1233. [PubMed: 24683502]
- [34]. Eslami S, Shang W, Li G, Patel N, Fischer GS, Tokuda J, Hata N, Tempany CM, and Iordachita I, “In-Bore Prostate Transperineal Interventions with an MRI-guided Parallel Manipulator: System Development and Preliminary Evaluation,” *Int J Med Robot*, vol. 12, no. 2, pp. 199–213, 2016. [PubMed: 26111458]
- [35]. Fry FJ, “Intense focused ultrasound in medicine,” *Eur. Urol*, vol. 23, no. Suppl. 1, pp. 2–7, 1993.
- [36]. Chang SD, Main W, Martin DP, Gibbs IC, and Heilbrun MP, “An analysis of the accuracy of the CyberKnife: a robotic frameless stereotactic radiosurgical system,” *Journal of Neurosurgery*, vol. 52, no. 1, pp. 140–6, 2003.
- [37]. Miller D, Smith N, Bailey M, Czarnota G, Hynynen K, and Makin I, “Overview of Therapeutic Ultrasound Applications and Safety Considerations,” *J Ultrasound Med.*, vol. 31, no. 4, pp. 623–634, 2012. [PubMed: 22441920]
- [38]. Masamune K, Kobayashi E, Masutani Y, Suzuki M, Dohi T, Iseki H, and Takakura K, “Development of an MRI-compatible needle insertion manipulator for stereotactic neurosurgery,” *J Image Guid Surg*, vol. 1, no. 4, pp. 242–248, 1995. [PubMed: 9079451]
- [39]. Starr PA, Martin AJ, Ostrem JL, Talke P, Levesque N, and Larson PS, “Subthalamic nucleus deep brain stimulator placement using high-field interventional magnetic resonance imaging and a skullmounted aiming device: technique and application accuracy,” *J Neurosurg*, vol. 112, no. 3, pp. 479–490, 2010. [PubMed: 19681683]
- [40]. Medtronic. [Online]. <http://www.medtronic.com/us-en/healthcare-professionals/products/neurological/laser-ablation/visualase.html>
- [41]. Monteris. [Online]. <https://www.monteris.com/our-technology/neuroblate-system/>
- [42]. Larson P, Starr PA, Ostrem JL, Galifianakis N, Palenzuela MSL, Martin A, “Application accuracy of a second generation interventional MRI stereotactic platform: initial experience in 101 DBS electrode implantations. *Neurosurgery*. 2013; 60:187,” *Neurosurgery*, vol. 60, no. CN_suppl_1, 2013.
- [43]. Li Gang, Su Hao, Cole Gregory A., Shang Weijian, Harrington Kevin, Camilo Alex, Pilitsis Julie G., and Fischer Gregory S., “Robotic System for MRI-Guided Stereotactic Neurosurgery,” *IEEE Trans Biomed Eng*, vol. 62, no. 4, pp. 1077–1088, 2015. [PubMed: 25376035]
- [44]. Varma T, Eldridge P, Forster A, Fox S, Fletcher N, Steiger M, Littlechild P, Byrne P, Sinnott A, and Tyler K, “Use of the NeuroMate stereotactic robot in a frameless mode for movement disorder surgery,” *Stereotactic and functional neurosurgery*, vol. 80, no. 1–4, pp. 132–135, 2004.
- [45]. Lang M, Greer A, and Sutherland G, “Intra-operative robotics: NeuroArm,” *Intraoperative Imaging*, vol. 109, pp. pp 231–236, 2011.
- [46]. Sutherland GR, Lama S, Shi Gan L, Wolfsberger S, and Zareinia K, “Merging machines with microsurgery: clinical experience with neuroArm,” *Journal of Neurosurgery*, vol. 118, no. 3, pp. 521–529, 2013. [PubMed: 23240694]
- [47]. Ho M, McMillan A, Simard J, Gullapalli R, and Desai J, “Toward a meso-scale SMA-actuated MRI-compatible Neurosurgical Robot,” *IEEE transactions on robotics*, vol. 99, pp. 1–10, 2011.
- [48]. Kim Y, Cheng SS, Diakite M, Gullapalli RP, Simard JM and Desai JP, “Toward the Development of a Flexible Mesoscale MRI-Compatible Neurosurgical Continuum Robot,” *IEEE Transactions on Robotics*, vol. 33, no. 6, pp. 1386–1397, 2017. [PubMed: 29225557]
- [49]. Comber DB, Barth EJ, and Webster RJ, “Design and control of an magnetic resonance compatible Precision Pneumatic Active Cannula Robot,” *Journal of Medical Devices*, vol. 8, 2014.
- [50]. Chen Y, Poorman ME, Comber DB, Pitt EB, Liu C, Godage IS, Yu H, Grissom WA, Barth EJ, and Webster RJ, “Treating Epilepsy via Thermal Ablation: Initial Experiments with an MRI-Guided Concentric Tube Robot,” in *Design of Medical Devices Conference*, Minneapolis, Minnesota, USA, 2017, p. V001T02A002.
- [51]. Comber D, Pitt EB, Gilbert HB, Powelson MW, Matijevich E, Neimat JS, Webster RJ, and Barth EJ, “Optimization of Curvilinear Needle Trajectories for Transforaminal Hippocampotomy,” *Operative Neurosurgery*, vol. 13, no. 1, pp. 15–22, 2016. [PubMed: 28580377]

- [52]. Nycz CJ, Gondokaryono R, Carvalho P, Patel N, Wartenberg M, Pilitsis JG, and Fischer GS, "Mechanical Validation of an MRI Compatible Stereotactic Neurosurgery Robot in Preparation for Pre-Clinical Trials," in IEEE/RSJ International Conference on Intelligent Robots and Systems (IROS), 2017, pp. 1677–1684.
- [53]. Nycz Christopher J, Gondokaryono Radian, Carvalho Paulo, Patel Nirav, Wartenberg Marek, Pilitsis Julie G, and Fischer Gregory S, "Mechanical validation of an MRI compatible stereotactic neurosurgery robot in preparation for pre-clinical trials," in Intelligent Robots and Systems (IROS), Canada, 2017.
- [54]. Heikkilä T, Yrjänä S, Kilpeläinen P, Koivukangas J, and Sallinen M, "An Assistive Surgical MRI Compatible Robot – First Prototype with Field Tests," InTech, vol. ISBN: 978–953-51–0623-4, 2012 Available from: <https://www.intechopen.com/books/explicative-cases-of-controversial-issues-in-neurosurgery/an-assistive-surgical-mri-compatible-robot-first-prototype-with-field-tests>.
- [55]. Song SE, Cho NB, Fischer G, Hata N, Tempany C, Fichtinger G, and Iordachita I, "Development of a Pneumatic Robot for MRI-Guided Transperineal Prostate Biopsy and Brachytherapy: New Approaches," in IEEE Int Conf on Robotics and Automation, 2010.
- [56]. Su H, Iordachita II, Yan X, Cole GA, and Fischer GS, "Reconfigurable MRI-Guided Robotic Surgical Manipulator: Prostate Brachytherapy and Neurosurgery Applications," in 33rd Annual International Conference of the IEEE EMBS, Boston, Massachusetts USA, 2011, pp. 2111–2114.
- [57]. "What are the key statistics about breast cancer? American Cancer Society. <http://www.cancer.org/cancer/breastcancer/detailedguide/breast-cancer-key-statistics>. Accessed 29 Apr 2016,".
- [58]. Ferlay J, Soerjomataram I, Dikshit R, Eser S, Mathers C, Rebelo M, Parkin DM, Forman D, and Bray F, "Cancer incidence and mortality worldwide: sources, methods and major patterns in GLOBOCAN 2012," *Int J Cancer*, vol. 136, no. 5, pp. E359–E386, 2015. [PubMed: 25220842]
- [59]. Park SB, Kim JG, Lim KW, Yoon CH, Kim DJ, Kang HS, and Jo YH, "A magnetic resonance image-guided breast needle intervention robot system: overview and design considerations," *Int J Comput Assist Radiol Surg*, vol. 12, no. 08, pp. 1319–1331, 2017. [PubMed: 28168682]
- [60]. Larson BT, Tsekos NV, and Erdman AG, "A Robotic Device For Minimally Invasive Breast Interventions With Real-Time MRI Guidance," in Third IEEE Symposium on Bioinformatics and Bioengineering, Bethesda, MD, USA, 2003.
- [61]. Kaiser WA, Fischer H, Vagner J, and Selig M, "Robotic system for biopsy and therapy of breast lesions in a high-field whole-body magnetic resonance tomography unit," *Investigative Radiology*, vol. 35, no. 8, pp. 513–519, 2000. [PubMed: 10946979]
- [62]. Yang B, Roys S, Tan UX, Philip M, Richard H, Gullapalli R, and JP Desai, "Design, development, and evaluation of a Master-Slave surgical system for breast biopsy under continuous MRI," *Int J Rob Res*, vol. 33, no. 4, pp. 616–630, 2014. [PubMed: 25313266]
- [63]. Chan KG, Fielding T, and Anvari M, "An image-guided automated robot for MRI breast biopsy," *Int J Med Robot*, vol. 12, no. 3, pp. 461–77, 2016. [PubMed: 27402476]
- [64]. Zhang T, Alarcon DN, Ng KW, Chow MK, Liu YH, and Chung HL, "A Novel Palm-Shape Breast Deformation Robot for MRI-Guided Biopsy," in IEEE International Conference on Robotics and Biomimetics (ROBIO), Qingdao, China, 2016.
- [65]. Navarro-Alarcon David, Singh Satwinder, Zhang Tianxue, Louise Chung Hayley, Wang Ng Kwun, Kiu Chow Man, and Liu Yunhui, "Developing a Compact Robotic Needle Driver for MRI-Guided Breast Biopsy in Tight Environments," *IEEE Robotics and Automation Letters*, vol. 2, no. 3, pp. 1648–1655, 2017.
- [66]. Groenhuis V, Siepel FJ, Veltman J, and Stramigioli S, "Design and characterization of Stormram 4: An MRI-compatible robotic system for breast biopsy," in IEEE/RSJ International Conference on Intelligent Robots and Systems (IROS), Vancouver, Canada, 2017, pp. 928–933.
- [67]. Zhang Y, Lu M and Du H, "Kinematics analysis and trajectory planning for a breast intervention robot under MRI environment," in IEEE International Conference on Cyborg and Bionic Systems (CBS), Beijing, 2017, pp. 237–242.
- [68]. Monfaredi R, Seifabadi R, Iordachita I, Sze R, Safdar NM, Sharma K, Fricke S, Krieger A, and Cleary K, "A prototype body-mounted MRI-compatible robot for needle guidance in shoulder

- arthrography,” Proc. IEEE RAS & EMBS Int. Conf. Biomedical Robotics and Biomechanics (BioRob), Sao Paulo, Brazil, pp. 40–45, 2014.
- [69]. Monfaredi R, Wilson E, Sze R, Sharma K, Azizi B, Iordachita I, and Cleary K, “Shoulder-Mounted Robot for MRI-guided arthrography: Accuracy and mounting study,” in International Conference of the IEEE Engineering in Medicine and Biology Society, Italy, 2015, pp. 3643–3646.
- [70]. Cleary K, Lim S, Jun C, Monfaredi R, Sharma K, Fricke ST, Vargas L, Petrisor D, and Stoianovici D, “Robotically Assisted Long Bone Biopsy Under MRI Imaging: Workflow and Preclinical Study,” *Academic Radiology*, vol. 25, no. 1, pp. 74–81, 2018. [PubMed: 29074334]
- [71]. Kim JS, Levi D, Monfaredi R, Cleary K and Iordachita I, “A new 4-DOF parallel robot for MRI-guided percutaneous interventions: Kinematic analysis,” in Annual International Conference of the IEEE Engineering in Medicine and Biology Society (EMBC), Seogwipo, 2017, pp. 4251–4255.
- [72]. Stoianovici D, Jun C, Lim S, Li P, Petrisor D, Fricke S, Sharma K, and Cleary K, “Multi-Imager Compatible, MR Safe, Remote Center of Motion Needle-Guide Robot,” *IEEE TRANSACTIONS ON BIOMEDICAL ENGINEERING*, vol. 65, no. 1, pp. 165–177, 2018. [PubMed: 28459678]
- [73]. Squires A, Oshinski JH, Boulis NM, and Tse ZTH, “SpinoBot: An MRI-Guided Needle Positioning System for Spinal Cellular Therapeutics,” in *Ann Biomed Eng.*, 2017, pp. 1–13.
- [74]. Melzer A, Gutmann B, Remmele T, Wolf R, Lukoscheck A, Bock M, Bardenheuer H, Fischer H, “INNOMOTION for percutaneous image-guided interventions: principles and evaluation of this MR- and CT-compatible robotic system,” *IEEE Eng Med Biol Mag*, vol. 27, no. 3, pp. 66–73, 2008.
- [75]. Miller JG, Li M, Mazilu D, Hunt T, and Horvath KA, “Robot-Assisted Real-Time Magnetic Resonance Image Guided Transcatheter Aortic Valve Replacement,” *J Thorac Cardiovasc Surg*, vol. 51, no. 5, pp. 1407–12, 2016.
- [76]. Li M, Kapoory A, Mazilu D, Woody B, and Horvath KA, “Cardiac Interventions under MRI Guidance using Robotic Assistance,” in *IEEE International Conference on Robotics and Automation (ICRA)*, Anchorage, AK, USA, 2010.
- [77]. Tavallaei MA, Thakur Y, Haider S, and Drangova M, “A Magnetic-Resonance-Imaging-Compatible Remot Catheter Navigation System,” *IEEE Transactions on Biomedical Engineering*, vol. 60, no. 4, pp. 899–905, 2013. [PubMed: 23192485]
- [78]. Franco E, Ristic M, Rea M, and Gedroyc WM., “Robot-assistant for MRI-guided liver ablation: A pilot study,” *Med Phys*, vol. 43, no. 10, 2016.
- [79]. Franco E, Brujic D, Rea M, Gedroyc WM, and Ristic M, “Needle-guiding Robot for Laser Ablation of Liver Tumors under MRI Guidance,” *IEEE/ASME Transactions on Mechatronics*, vol. 21, no. 2, pp. 931–944, 2016.
- [80]. “ASTM F2503–13, Standard Practice for Marking Medical Devices and Other Items for Safety in the Magnetic Resonance Environment”.
- [81]. Fischer GS, Cole G, and Su H, “Approaches to Creating and Controlling Motion in MRI,” in *Conf Proc IEEE Eng Med Biol Soc*, Boston, MA, USA, 2011, pp. 6687–90.
- [82]. Shokrollahi Peyman, Drake James M., and Goldenberg Andrew A., “Quantification of Force and Torque Applied by a High-Field Magnetic Resonance Imaging System on an Ultrasonic Motor for MRI-Guided Robot-Assisted Interventions,” *Actuators*, vol. 6, no. 4, 2017.
- [83]. Gassert R, Yamamoto A, Chapuis D, Dovat L, Bleuler H, and Burdet E, “Actuation Methods for Applications in MR Environments,” *Concepts in Magnetic Resonance Part B: Magnetic Resonance Engineering*, vol. 29B, no. 4, pp. 191–209, 2006.
- [84]. Gassert R, Moser R, Burdet E, and Bleuler H, “Mri/fmri-compatible robotic system with force feedback for interaction with human motion,” vol. 11, pp., April 2006., *IEEE Trans Mech*, vol. 11, pp. 216–224, 2006.
- [85]. Fischer GS, Krieger A, Iordachita I, Csoma C, Whitcomb LL, and Fichtinger G, “MRI Compatibility of Robot Actuation Techniques – A Comparative Study,” in *International Conference on Medical Image Computing and Computer-Assisted Intervention*, 2008, pp. 509–517.

- [86]. Vartholomeos P, Bergeles C, Qin L, and Dupont PE, “An MRI-powered and controlled actuator technology for tetherless robotic interventions,” *The International Journal of Robotics Research*, vol. 32, no. 13, pp. 1536–1552, 2013.
- [87]. Ouchi R, Saotome K, Matsushita A, and Suzuki K, “Development of an MRI-powered robotic system for cryoablation,” in *IEEE 37th Annual International Conference of Engineering in Medicine and Biology Society (EMBC)*, Milan, Italy, 2015, pp. 1186–1189.
- [88]. Monfaredi R, Seifabadi R, Fichtinger G, Iordachita I, “Design of a decoupled MRI-compatible force sensor using fiber Bragg grating sensors for robot-assisted prostate interventions,” in *Image-Guided Procedures, Robotic Interventions, and Modeling: Medical Imaging*, 2013, p. Vol. 8671.
- [89]. Seifabadi R, Aalamifar F, Iordachita I, and Fichtinger G, “Toward teleoperated needle steering under continuous MRI guidance for prostate percutaneous interventions,” *The International Journal Of Medical Robotics and Computer Assisted Surgery*, vol. 12, pp. 355–369, 2016. [PubMed: 26264564]
- [90]. Su H, Iordachita I, Tokuda J, Hata N, Liu X, Seifabadi R, Xu S, Wood B, and Fischer GS, “Fiber-Optic Force Sensors for MRI-Guided Interventions and Rehabilitation: A Review,” *IEEE Sensors Journal*, vol. 17, no. 7, pp. 1952–1963, 2017. [PubMed: 28652857]
- [91]. Shellock FG, and Cruess JV, “MR Safety and the American College of Radiology,” *American Journal of Roentgenology*, vol. 178, no. 6, pp. 1349–1352, 2002. [PubMed: 12034595]
- [92]. Fischer GS, Cole G, and Su H, “Approaches to creating and controlling motion in MRI,” in *IEEE Eng. Med. Biol. Soc. Conf*, 2011, pp. 6687–6690.
- [93]. Tokuda J, Song SE, Tuncali K, Tempny C, and Hata N, “Configurable Automatic Detection and Registration of Fiducial Frames for Device-to-Image Registration in MRI-guided Prostate Interventions,” *Med Image Comput Comput Assist Interv*, vol. 16, no. 03, pp. 355–362, 2013. [PubMed: 24505781]
- [94]. Shang W, and Fischer GS, “A high accuracy multi-image registration method for tracking MRI-guided robots,” in *Image-Guided Procedures, Robotic Interventions, and Modeling*, 2012.
- [95]. Tokuda J, Fischer GS, DiMaio SP, Gobbi DG, Csoma C, Mewes PW, Fichtinger G, Tempny CM, and Hata N, “Integrated navigation and control software system for MRI-guided robotic prostate interventions,” *Computerized Medical Imaging and Graphics*, vol. 34, no. 1, pp. 3–8, 2010. [PubMed: 19699057]
- [96]. Gering DT, Nabavi A, Kikinis R, Hata N, O’Donnell LJ, Grimson WE, Jolesz FA, Black PM, Wells WM, “An integrated visualization system for surgical planning and guidance using image fusion and an open MR. 2001; 13: pp. 967–975,” *J Magn Reson Imaging*, vol. 13, pp. 967–975, 2001. [PubMed: 11382961]
- [97]. Stoianovici D, Jun C, Lim S, Li P, Petrisor D, Fricke S, Sharma K, and Cleary K, “Multi-Imager Compatible, MR Safe, Remote Center of Motion Needle-Guide Robot,” *IEEE TRANSACTIONS ON BIOMEDICAL ENGINEERING*, vol. TBD, no. TBD, 2017.
- [98]. Intuitive Surgical Inc. [Online].http://www.davincisurgery.com/da-vinci-surgery/da-vinci-surgical-system/?gclid=Cj0KCQiA-qDTBRD-ARIsAJ_10yJhiGRLKRZKAR_e0CQWLdEULMXmwy2DPWhoN4VLQpNknAJffb0Y24aAjN-XEALw_wcB
- [99]. Cleary K, and Kinsella A, “The Operating Room of the Future,” Department of Radiology, Georgetown University, Washington DC, Workshop Report <http://www.dtic.mil/dtic/tr/fulltext/u2/a430482.pdf>.
- [100]. Giannarini G, Zazzara M, Rossanese M, Palumbo V, Pancot M, Como G, Abbinante M, and Ficarra V, “Will multi-parametric magnetic resonance imaging be the future tool to detect clinically significant prostate cancer?,” *Front. Oncol*, 04 November 2014.
- [101]. Riffel P, Rao RK, Haneder S, Meyer M, Schoenberg SO, and Michaely HJ, “Impact of Field Strength and RF Excitation on Abdominal Diffusion-weighted Magnetic Resonance Imaging,” *World J Radiol*, vol. 5, no. 9, pp. 334–344, 2013 9 28. [PubMed: 24198912]
- [102]. McClure Ashley, “Using High-Intensity Focused Ultrasound as a Means to Provide Targeted Drug Delivery: A Literature Review,” *Journal of Diagnostic Medical Sonography*, vol. 32, no. 6, pp. pp. 343–350, 2016.

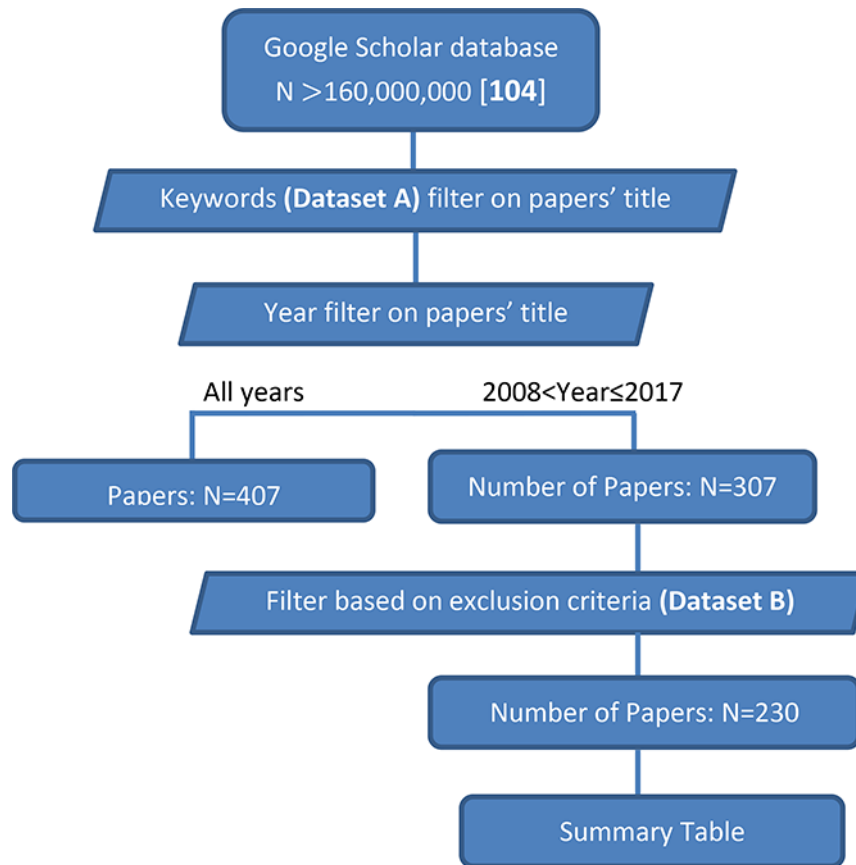


Fig. 1.
Diagram of systematic review

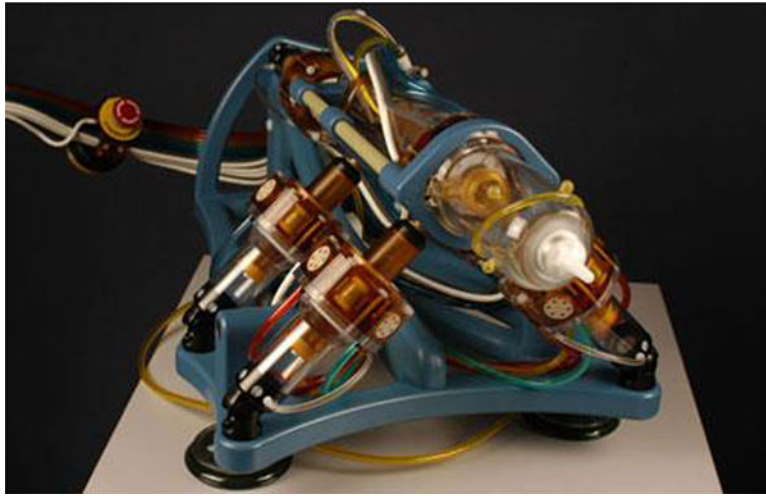


Fig. 2.
The MrBot robot is a fully pneumatically actuated robot developed for MRI-guided prostate biopsy [18]

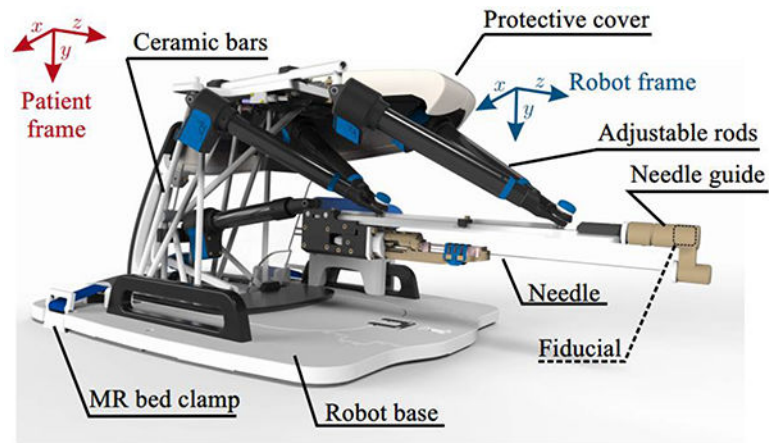


Fig. 3. The MIRIAM robot, a novel robotic system for MR-guided needle insertion for prostate biopsy [21]

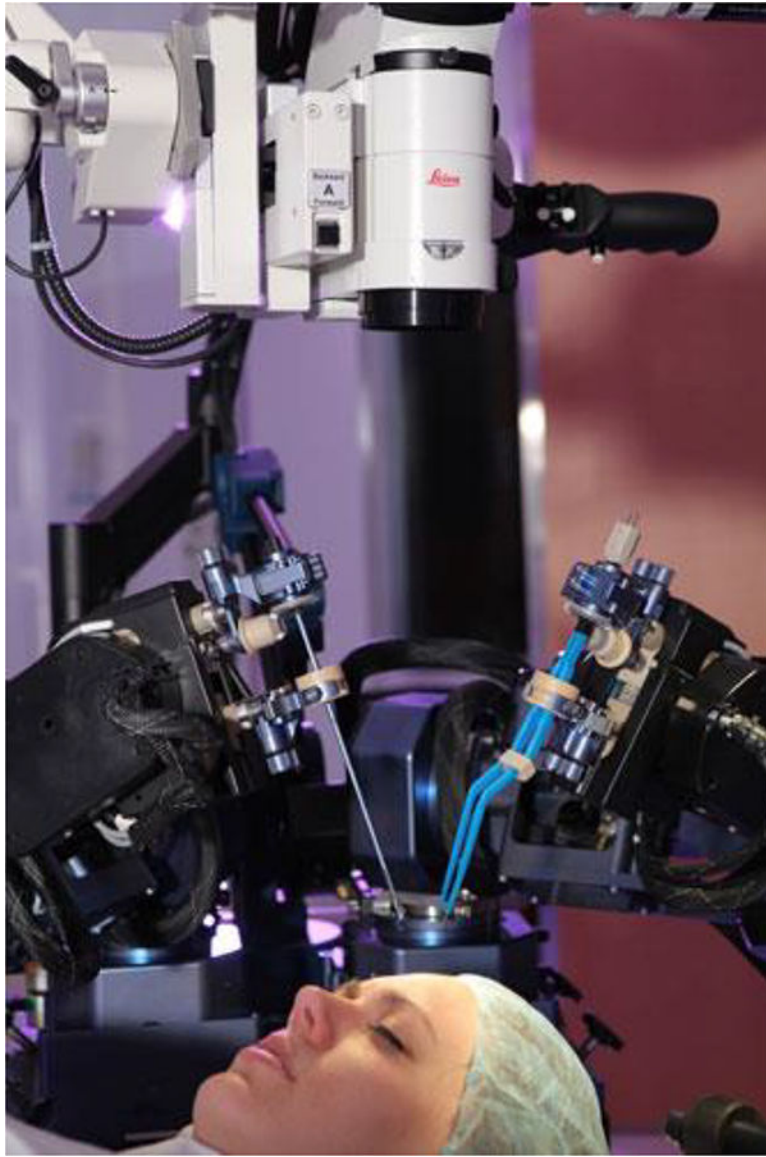


Fig. 4. The NeuroArm robot in a MRI room with dual dexterous arms (Image source: <http://www.neuroarm.org/project/>) [45]

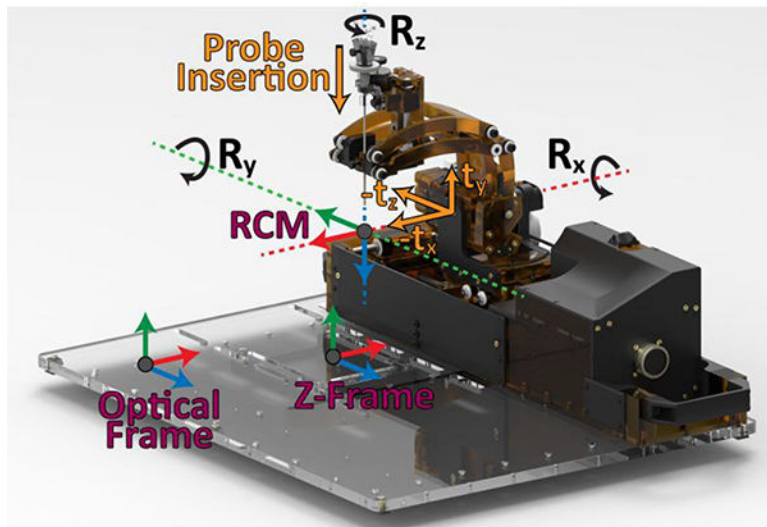


Fig. 5. A Stereotactic neurosurgery MRI robot which is kinematically equivalent to a Leksell frame [43]

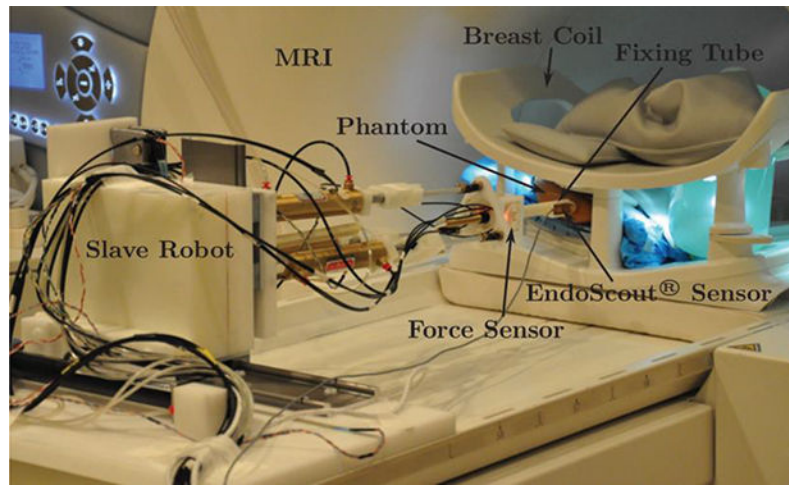


Fig. 6.
A master-slave MRI robot; slave robot is shown on a MRI scanner table [62]

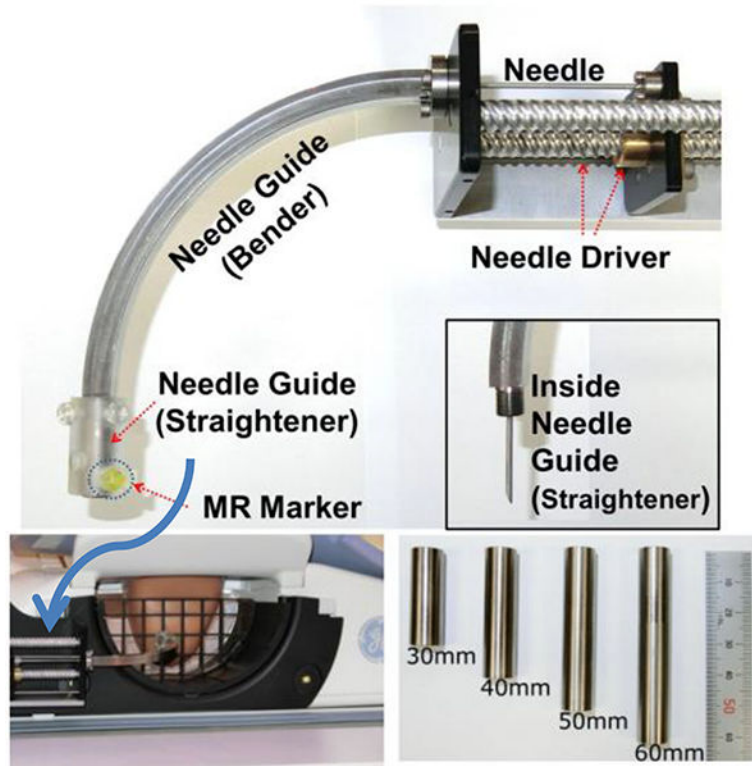


Fig. 7. An automated bendable needle intervention robotic system for MRI-guided breast biopsy [59]

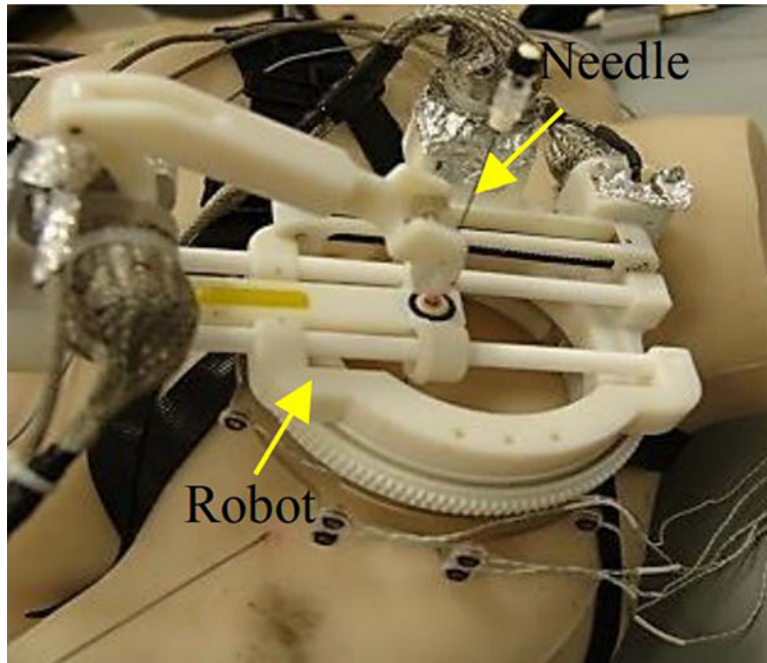


Fig.8. A patient-mounted MRI robot with 4 DOF for shoulder arthrography procedure [68] [69]

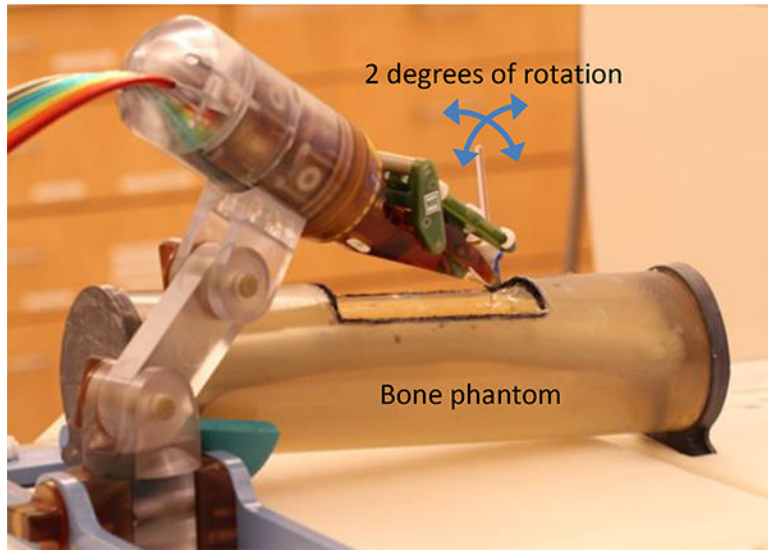


Fig. 9.
A 2 DOF pneumatic MRI robot for bone biopsy [65].

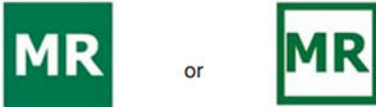


Icon Geometric Shape and Appearance	Meaning
<p>A square</p> 	MR Safe
<p>An equilateral triangle with radiused outer corners</p> 	MR Conditional
<p>A circle with a diagonal bar</p> 	MR Unsafe

Fig. 10. Colored MR Icons for labeling equipment in MRI environment suggested in standard F2503–13 [80]

Table 1:

MRI robotic system for prostate intervention that are in phantom study phase

Year	Team	Study type	Accuracy	DOF	Actuation type	Control type	SNR	Design	Institute
2010	Bosch et al. [13]	Clinical study (N=1)	Needle Insertion accuracy < 1mm	6 DOF	Pneumatic and hydraulic	Automatic needle insertion	-	-	University Medical Center Utrecht
2010	Xu et al. [15]	Clinical study (N=21)	4 mm Mean 2 mm SD	3 DOF	Passive device	Remote- manual control	-	Passive	Queen's University
2011	Böstrom et al. [16]	Clinical study (N=2)	3 mm	-	-	-	-	The robot consists of a motorized trajectory alignment (TA) unit	Toronto, Canada
2012	Schouten et al. [17]	Clinical study (N=13) (T=32)	6.5 mm	5 DOF	Pneumatic	Interactive image guidance	-	Table mounted robot	Radboud University
2017	Ball et al. [18]	Clinical study (N=5)	2.55 mm	6 DOF	PneuStep	-	-	5 DOF parallel robot 1 DOF needle drive	Johns Hopkins University
2014	Srimathveeravalli et al. [19]	Animal study (N=6)	Mean 2.58 mm	3 DOF	PneuStep	-	Mean value of 9.99 with a SD of 2.88	2 DOF needle orientan 1 DOF passive needle insertion	Memorial Sloan-Kettering Cancer Center
2017	Chen et al. [22]	Canine Cadaver	0.9 mm; 0.4 SD mm	2 DOF	Pneumatic turbine Motors	-	-	-	University of Georgia
2013	Jiang et al. [23]	Only design is reported	-	5 DOF	Ultrasonic motors	-	-	3 DOF positioner 3 D needle drive	-
2013	Li et al. [24] Hao et al. [25]	Phantom	0.98mm RMS 0.37mm SD	6 DOF	Non-harmonic piezoelectric motor	Interactive MRI guidance	No significant signal degradation with a 95% confidence interval	Modular design for various application	Worcester Polytechnic Institute
2013	Song et al. [26] Tokuda et al. [27] Song et al. [28]	Saline phantoms patient mockup	0.8 ± 0.5 mm horizontally 0.8 ± 0.8 mm vertically	4 DOF	Pneumatically actuated	-	15% SNR reduction	Parallel kinematic structure	Brigham & Women's Hospital
2013	Krieger et al. [29]	Phantom	in-plane targeting error of 2.4 mm	2 DOF	Piezo-ceramic-motor	-	40% to 60% drop with RF shielding	Mounted on 6 DOF passive mounting arm	Johns Hopkins University
2015	Su et al. [30]	Phantom	0.87 mm RMS	6 DOF	Piezoelectric motor	Interactive MRI guidance	15% Loss	3 DOF needle driver and a 3 DOF Cartesian motion	-
2015	Chen et al. [31]	-	0.6 mm	5 DOF	Novel Pneumatic Motors	-	-	Parallel	Fraunhofer MEVIS
2015	Yiallouras et al. [32]	Phantoms	Positioning: 25 µm Rotation: 0.11o	3 DOF	piezoelectric motors	PC-controlled axes	Max 28%	-	City University

Author Manuscript

Author Manuscript

Author Manuscript

Author Manuscript

Year	Team	Study type	Accuracy	DOF	Actuation type	Control type	SNR	Design	Institute
2016	Eslami et al. [33] [34]	In air	1 mm	4 DOF	Piezoelectric actuators	-	-	Parallel robot	Johns Hopkins University
2017	Moreira et al. [21]	Phantom	Average targeting error of 1.84 mm	9 DOF	Piezoelectric; pneumatic for firing the needle	-	SNR reduction of 25%	Steer and fire a biopsy needle	University of Twente

Table 2:

MRI robotic system for neurosurgical intervention

Year	Team	Study type	Accuracy	DOF	Actuation type	Control type	SNR	Design	Institute
2011	Lang et al. [45] [46]	Clinical study (N=35)	-	8 DOF	-	-	-	2 arms	University of Calgary
2014	Comber et al. [49]	In air	mean of 0.032 mm and 0.447 deg	5 DOF	Pneumatic	-	0.7 % drop	-	Vanderbilt University
2015	Li et al. [43] [30]	Phantom	Tip pose: 1.38 ± 0.45 mm; Insertion angle 2.03 ± 0.58°	5 DOF	PiezoLegs motors	-	Less than 15% SNR reduction	Kinematically equivalent to the commonly used Leksell stereotactic frame	Worcester Polytechnic Institute
2015	Ho et al. [48] [103]	Phantom	RMS 0.21°	4 DOF	Shape memory alloy (SMA)	Image feedback control	SNR dropped by 0.7% during actuation Or dropped by about 10% [Ho et al 2012]	Finger link robot	University of Maryland
2017	Kim et al. [47]	Phanto	-	6 DOF	Shape memory alloy (SMA)	-	6.4% SNR drop During actuation	Finger link robot	University of Maryland
2017	Chen et al. [50]	Phantom	Mean 0.47 mm	-	Pneumatic actuators	-	-	Concentric Tube Robot helical steerable needle	Vanderbilt University
2017	Nyeç et al. [53]	-	Tip pose: 1.37 ± 0.06 mm; Insertion angle 0.79° ± 0.41°	7 DOF	piezoelectric ultrasonic motors	Automated needle drive	2.9% SNR drop (Powered on) 10.3% SNR drop (moving)	Kinematically equivalent to the commonly used Leksell stereotactic frame	Worcester Polytechnic Institute

Table 3:

MRI robotic system for breast cancer intervention

Year	Team	Study type	Accuracy	DOF	Actuation type	Control type	SNR	Design	Institute
2014	Yang et al. [62]	Animal study	The target was reached in total of 50 minutes	6 DOF	5 pneumatic cylinders 1 Piezomotor	Interactive MRI master-slave	Less than 8% drop	5 DOF robot 1 DOF needle drive	University of Maryland
2016	Chan et al. [63]	In air	0.34 mm	6 DOF	Piezoelectric motors	-	13% drop in 1.5 Tesla 2.5% drop in 3.0 Tesla	3 subsystems: the manipulator, a toolset, and a patient support	McMaster University
2017	Park et al. [59]	Phantom	2.3 mm	4 DOF	Piezoelectric motors	Automated needle drive	acceptable for manual and automatic image segmentation	Bendable needle curved trajectory	National Cancer Center Republic of Korea
2017	Navarro-Aliarcon et al. [65]	Phantom	± 0.4 mm x and y And ± 1.5 mm insertion	3 DOF	Piezo motors and pneumatic actuators	Automated needle drive	No significant degradation of the MR images	Cartesian mechanism	The Chinese University of Hong Kong
2017	Groenhuis et al. [66]	In air	Mean 0.7 mm, with a reproducibility of 0.1 mm	4 DOF	Linear and curved pneumatic stepper motors	Manual mode and automatic mode	-	Serial kinematic chain	University of Twente
2017	Zhang et al. [67]	Phantom	-	7 DOF	Flexible shafts and remote DC motors	-	-	Positioning module (4 DOF) Puncturing module Biopsy module Storage module	School of Harbin University of Science and Technology

Table 4:

MRI robotic system for other needle-based intervention

Year	Team	Study type	Accuracy	DOF	Actuation type	Control type	SNR	Institute	Application
2016	Miller et al. [75]	Nonsurvival swine study (N=8)	All stents were deployed successfully	-	Innomotion	-	-	National Institutes of Health (NIH), USA	Cardiac intervention
2010	Li et al. [76]	Ex-vivo	0.8 mm and 1.5 mm	-	Innomotion	-	-	National Institutes of Health (NIH), USA	Cardiac intervention
2013	Tavallaei et al. [77]	In air	$2 \pm 2\sigma$ rotation 1.0 ± 0.8 mm axial	2 DOF	ultrasonic motor	Master-slave	Less than 2.5% drop	University of Western Ontario	Cardiac catheterization
2015	Monfaredi et al. [68] [69]	Phantom	-	4 DOF	Piezoelectric motor	Manual needle insertion	Powered off: 2% drop	Children's National Health System, DC, USA	Arthrography
2016	Franco et al. [78] [79]	Phantom	Below 5 mm	4 DOF	Pneumatic cylinders	Manual needle insertion	Less than 5% drop	Imperial College London	Liver tumor ablation
2017	Kim et al. [71]	-	-	4 dof	Piezoelectric motor	Manual needle insertion	-	Johns Hopkins University	Arthrography
2017	Stoianovici et al. [72]	Phantom	1.39 mm SD 0.4 mm	3 DOF	PneuStep	Manual tool insertion	-	Children's National Health System, DC, USA Johns Hopkins university	Bone biopsy
2017	Squires et al. [73]	Swine Cadaver	1.12 mm SD 0.97 mm	4 DOF	Pneumatic motor	-	Less than 3% in 3 a Tesla scanner	University of Georgia	Spinal Cellular Therapeutics